14B.2 THE RELATIONSHIP BETWEEN THE MJO, OCEANIC KELVIN WAVES, AND THE EL NIÑO/SOUTHERN OSCILLATION

Paul E. Roundy* and George N. Kiladis
NOAA/CIRES Aeronomy Laboratory
Boulder, Colorado

1. Introduction

The Madden Julian Oscillation (MJO), oceanic Kelvin waves, and the El Niño/Southern Oscillation (ENSO) follow a systematic pattern of feedbacks that control the amplitude, structures, and other variability of each mode. Though some of these interactions are well understood (Kessler et al. 1995; Hendon et al., 1998; Zhang, 2001), there is still dispute over many of the details. For example, there is not yet a consensus about whether synoptic scale westerly wind bursts (WWBs) or the MJO are most effective in producing the 70-day Kelvin wave that occurs in the equatorial Pacific basin.

We describe a linear regression model that diagnoses the relationships between background convection, equatorial zonal wind stress, the dynamic height of the ocean surface, the sign and trend of ENSO, and an index for oceanic Kelvin waves at the date line. This model clearly indicates the structure of the forcing that produces the oceanic Kelvin waves, and how that structure changes with ENSO phase.

2. Data and Methods

We analyze all available wind, SST, and ocean surface dynamic height data from the TAO buoy array along with OLR data for the period 1988-2003. Missing TAO data from each buoy were interpolated by multiple linear regression based on the set of nearest neighboring buoys. An index for ENSO was developed from the dynamic height data by averaging over the Nino 3.4 region and subjecting the data to a 200-day low-pass filter. The dynamic height was selected because it is more directly related to the atmospheric forcing than is SST. An index for the 70-day oceanic Kelvin wave was developed by filtering dynamic height data at the equator and the date line for the 20-100 day band. A tendency series was developed for the ENSO index by taking its first time differential.

Multiple linear regression models were developed for OLR, SST, and winds at each grid point. These models are based on the Kelvin wave index. They also include the second through fourth powers of the Kelvin wave index, ENSO modulation terms (the product of a selected ENSO index and the Kelvin wave index), and modulation by the ENSO tendency (the product of the ENSO tendency index and the Kelvin wave index). The first through third powers of the modulation terms were also included in the model. The higher powers are useful because they diagnose relationships that occur across different frequencies. The set of predictors were orthogonalized by following the Graham Schmidt process to remove collinearities between the predictors. Regression coefficients were found for each grid point and for a range of time lags. Next, composites were developed by substituting values for each predictor. The purpose of these substitutions was to generate composites of the relationships between the OLR, winds, and the oceanic Kelvin waves during different phases of ENSO. Values included 2 standard-deviations (STDs) above the mean for the Kelvin wave index (corresponding to a wave crest at the date line), 1 STD above and below the mean for the ENSO index (hereafter labeled warm or cold, respectively), and 2 STDs above and below the mean for the ENSO trend index (hereafter labeled warming and cooling, respectively). The value of the standard deviation of the Kelvin wave index was calculated from subsets of the time series during which the ENSO index was above average and increasing with time, above average and decreasing, below average and decreasing, and below average and increasing. The Kelvin wave activity varies tremendously with ENSO phase, so using the STD for the entire time series for every case would be inappropriate. The resulting composites reveal much about how the structures of the Kelvin waves and their atmospheric forcing change with ENSO phase and trend.

3. Results and Discussion

Figures 1-4 show the composite results for OLR, dynamic height, and the zonal component of the surface wind stress (calculated from the composite winds). For reference, Figure 1 shows a composite regressed against the Kelvin wave index using all data in which all ENSO modulation is ignored. Note the differing phase speeds of the OLR and dynamic height anomalies. These figures indicate that as warm events develop (Figure 2), 70-day Kelvin waves are forced by a 40-50 day oscillation similar to the MJO that is seen both in OLR and in the TAO wind stress. These Kelvin waves then propagate as free waves across the Pacific. Figure 3 shows that when the ENSO index is consistent with a weakening warm event, the frequency of the OLR signal is higher than it was during the strengthening phase. Additionally, as the warm event weakens, the structure of the wind stress changes such that Kelvin waves are initially forced over the western Pacific, but subsequently destroyed as they propagate into the central Pacific where the forcing occurs ahead of the wave (not shown). This destructive forcing prevents the waves from reaching the East Pacific with any appreciable amplitude. During the ENSO cold and cooling stage (Figure 4), the MJO disturbs the west Pacific, but Kelvin waves do not tend to cross the date line. This phase of ENSO is characterized by a lack of Kelvin wave activity in the East Pacific. The cold and warming stage (not shown) is characterized by Kelvin waves that undergo weak but constructive forcing, which allows them to begin crossing the basin again.

* Correspondence: Paul Roundy, NOAA/CIRES Aeronomy Laboratory, 325 Broadway, Boulder, CO 80305. proundy@al.noaa.gov

The results indicate that the structure of the anomalies that force the oceanic Kelvin waves is similar at large scales to the MJO, but it also contains some synoptic scale features similar to WWBs (not shown). This analysis shows that the structure and frequency of the atmospheric forcing changes with ENSO phase, allowing for constructive Kelvin wave forcing during the onset stage of a warm event, followed by destructive forcing as the dynamic height anomaly of the warm event approaches its peak and begins to decline. These and other results suggest that a the ocean needs to be prepared in advance of a warm event by storing sufficient heat in the western part of the basin (consistent with Jin, 2001) in order to improve the local air-sea coupling of the MJO, but thereafter, formation, ultimate amplitude, and decay of the event may be explained primarily by changes in the structure and frequency of the atmospheric forcing alone.

References

Hendon, H.H., B. Liebmann, and J.D. Glick, 1998: Oceanic Kelvin waves and the Madden-Julian Oscillation. *J. Atmos. Sci.,* **55**, 8-101.

Jin, F., 1997: An equatorial ocean recharge paradigm for ENSO. Part I: conceptual model. *J. Atmos. Sci*., **54**, 811-829.

Kessler, W.S., and R. Kleeman, 2000: Rectification of the Madden-Julian Oscillation into the ENSO cycle. *J. Climate*, **13**, 3560-3575.

Zhang, C., and J. Gottschalck, 2002: SST anomalies of ENSO and the Madden-Julian Oscillation in the equatorial Pacific. *J. Climate*, **15**, 2429-2445.

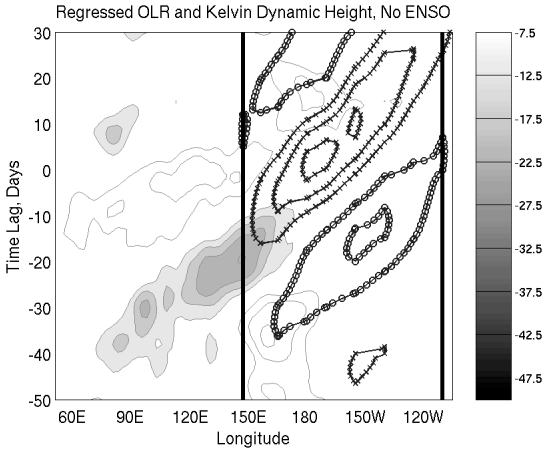

Figure 4 Longitude-time lag composite equatorial OLR (shaded and with fine contours), oceanic Kelvin wave band dynamic height (positive contours marked with x, negative marked with o.

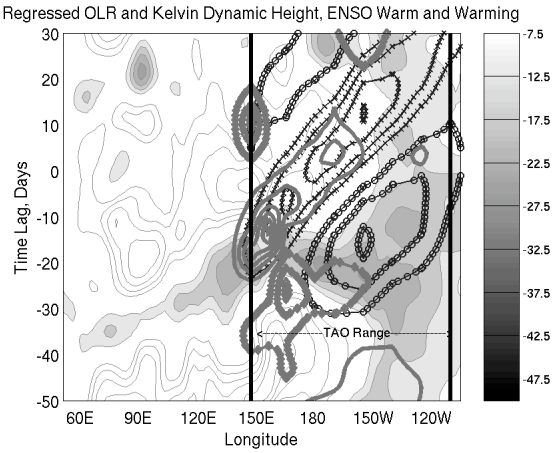

Figure 2 Same as Figure 1, except for Nino 3.4 dynamic height consistent with ENSO warm and warming. Zonal wind stress is also included (positive contours heavy, negative contours with diamonds).

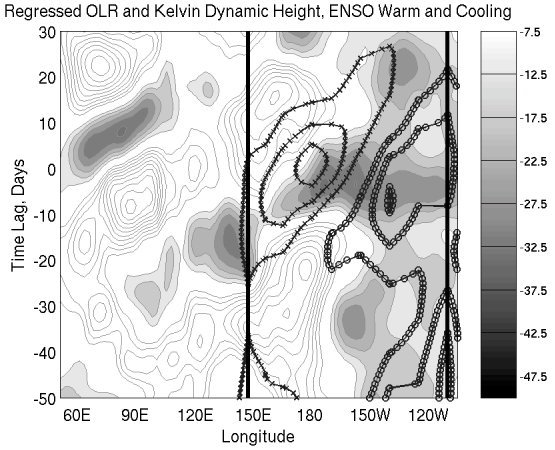

Figure 3 Same as Figure 1, except for ENSO index consistent with warm and cooling Nino 3.4 conditions.

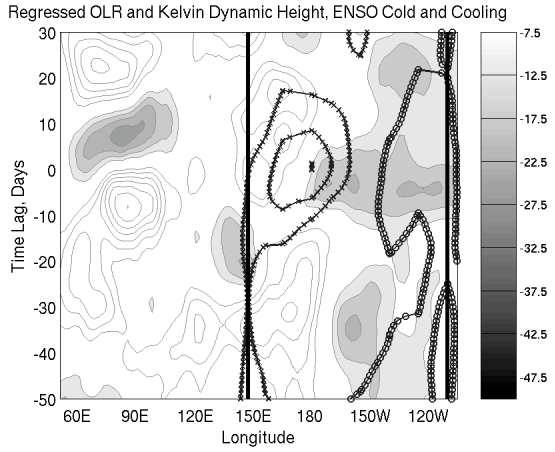

Figure 4 Same as Figure 1, except for ENSO cold and cooling.